Supporting Information for

Guest-conditioned Multicolor Writing on Cellulose Nanocrystal Canvases

Miguel A. Soto,[a⊥] Dongjie Zhang,[ab⊥] Yitao Xu,[a] Yihan Shi,[a] Brian Patrick,[a] Wadood Y. Hamad,[c] and Mark J. MacLachlan*[ade]

[a] Department of Chemistry, University of British Columbia, 2036 Main Mall, Vancouver, British Columbia V6T 1Z1, Canada

[b] MIIT Key Laboratory of Critical Materials Technology for New Energy Conversion and Storage, School of Chemistry and Chemical Engineering, Harbin Institute of Technology, Harbin 150001, P. R. China

[c] Transformation and Interfaces Group, Bioproducts, FPInnovations, 2665 East Mall, Vancouver, British Columbia V6T 1Z4, Canada

[d] Stewart Blusson Quantum Matter Institute, University of British Columbia, 2355 East Mall, Vancouver, BC, V6T 1Z4 Canada

[e] WPI Nano Life Science Institute, Kanazawa University, Kanazawa, 920-1192 Japan

[⊥] These authors contributed equally

Contents

General

Aqueous suspensions of cellulose nanocrystals (CNCs) were provided by FPInnovations as the sodium-neutralized form (CNC-Na^+, 6 wt%, pH 6) and were prepared by a previously reported method.[1] In brief, spray-dried CNCs were mechanically stirred overnight in deionized water at a concentration of 2 wt %. An ultrasonicator Vibra-Cell VC 750 (Sonics & Materials Inc.) was used to sonicate the CNC suspension in 3 L batches for 30 min at 70% power, which corresponds to an average energy input of ~9000 J/g of CNC. The suspension was then filtered through grade 4 Whatman filter paper, followed by grade 42 Whatman filter paper, and then dialyzed overnight against deionized water. The desired concentration was adjusted using a rotary evaporator, and NaOH was used to adjust the pH and conductivity of the ultrapure CNC aqueous suspension (CNC-Na^+, pH 6) followed by filtration. CNC suspensions were stored at 4 °C until further use. The typical dimensions of CNC spindles were determined by transmission electron microscopy to be 191 ± 80 nm by 13 ± 3 nm. Deuterated solvents (D_2O and DMSO-d_6) were purchased from Cambridge Isotope Laboratories and Sigma-Aldrich. Nuclear magnetic resonance (NMR) experiments were recorded on Bruker AVIII HD 400 MHz and Bruker Avance 400 MHz spectrometers; ^{1}H NMR chemical shifts (δ) are given in parts per million (ppm) relative to TMS (using the residual solvent signal as an internal reference). UV-vis and transmittance spectra were recorded on a Cary 5000 UV-vis-NIR spectrophotometer employing 1.0 cm path length quartz cuvettes. Reflectance experiments were performed in an Ocean Optics Flame miniature spectrometer, using a UV-vis reflection probe. Scanning electron micrographs were capture with a Hitachi S-4700 Field Emission electron microscope. Thermogravimetric analyses were performed in a TG 209 F3 Tarsus instrument from Netzsch.

Guests **G1** (phenol), **G2** (indole), and **G4** (1,5-diaminonaphthalene) were purchased from Sigma-Aldrich and used without further purification. Compound **M1**,[2] Guests **G3** (1,4-bis[2-(2-hydroxyethoxy)ethoxy]benzene),[2] **G5** (1,5-bis[2-(2-hydroxyethoxy)ethyloxy]naphthalene),[2] and **G6** (1,5-bis[2-(2-hydroxyethoxy)ethylamino]naphthalene)[3] were synthesized following reported methodologies, as well as the chloride salt of cyclobis(paraquat-*p*-phenylene) (**CBPQT**$^{4+}$).[2] In all cases, the spectroscopic characterization matched with the reported data.

Film preparation

Gels were assembled by mixing an aqueous CNC suspension (CNC-Na^+, 6 wt%, pH = 6) with [**CBPQT**]Cl_4 (50 mM in water) in a glass vial, followed by shaking and sonication until getting a homogeneous gel material (typically 2 h). Final concentrations of **CBPQT**$^{4+}$ were set to 1.3, 2.5, and 3.8 and 7.0 mM. All resulting samples (CNC-**CBPQT**$^{4+}$) were then casted on a polypropylene substrate (5 × 1 cm) and air-dried at room temperature overnight Scheme S1. The films were washed with ethanol/water (10 mL, 3/1, v/v). The resulting materials were air-dried again and stored in sealed vials at room temperature prior to usage.

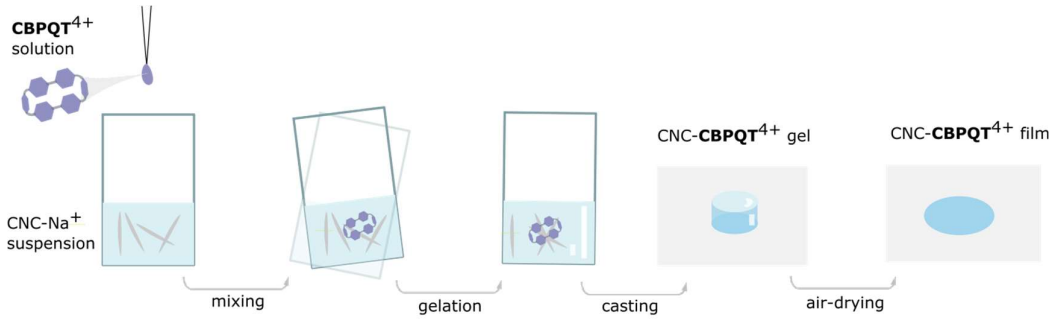

Scheme S1. Preparation of CNC-**CBPQT**$^{4+}$ gel and film receptors.

Film characterization

The effect of host concentration on all resulting CNC-**CBPQT**$^{4+}$ films was investigated through UV-vis spectroscopy, scanning electron microscopy (SEM), and thermogravimetric analysis (TGA).

UV-vis spectroscopy

The CNC-**CBPQT**$^{4+}$ films were mounted on a sample holder and examined by UV-vis spectroscopy using transmission mode. Figure S1 shows representative results for materials composed of 1, 2, 3 and 7 %wt of host.

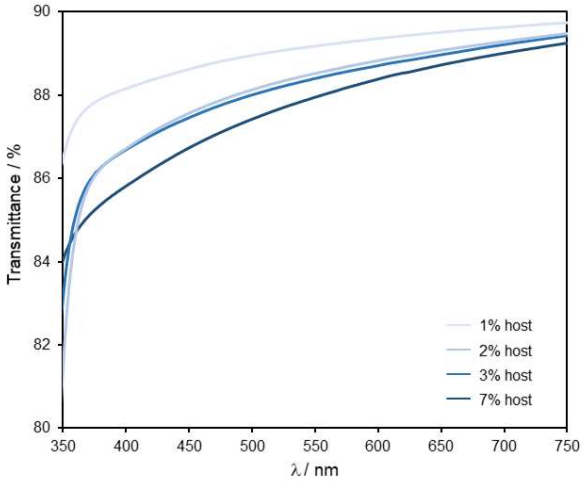

Figure S1. Transmittance plot for a series of CNC-**CBPQT**$^{4+}$ films composed of varied amounts of host.

Thermogravimetric analysis

Figure S2 shows the TGA traces of three representative films containing 1, 3 and 7 wt% of host.

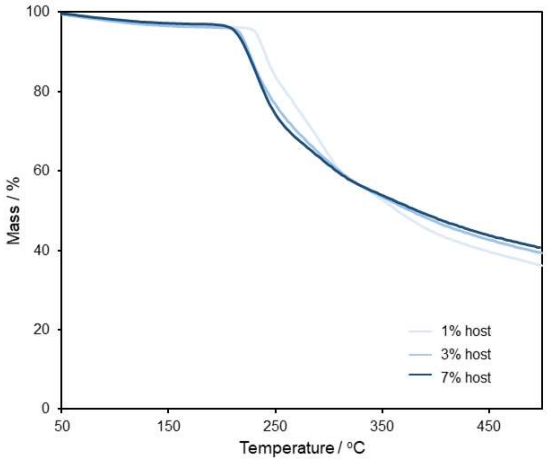

Figure S2. TGA traces of a series of CNC-**CBPQT**$^{4+}$ films containing varied amounts of host. All samples were run under a N_2 atmosphere at a heating rate of 10 ºC/min.

Scanning electron microscopy

Figure S3 shows the SEM images of both surface and cross sections of a series of films.

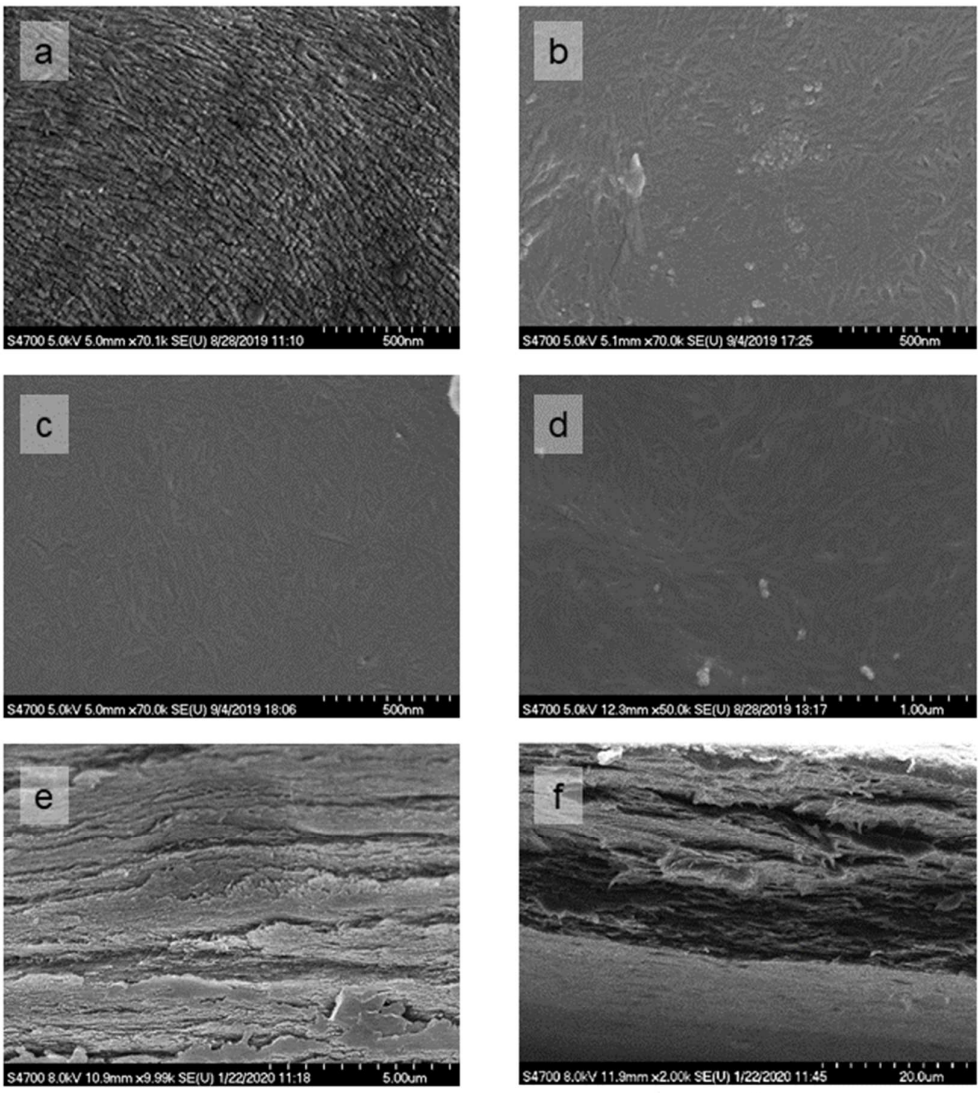

Figure S3. SEM images showing the surface features of films containing (a) 1 wt%, (b) 2 wt%, (c) 3 wt%, and (d) 4 wt% of host. Micrographs (e) and (f) show the cross section of films composed of 2 wt% and 7 wt% (host), respectively.

Film stability in D_2O

A CNC-**CBPQT**$^{4+}$ film (10 mg, 7 wt% host) was added into an NMR tube which was previously loaded with a concentration reference (capillary tube containing 5 mM hydroquinone in DMSO-d_6). D_2O (400 mL) was then added, and the system was stored at room temperature for 3 months. Figure S4 shows a ^{1}H NMR spectrum collected after this storage period.

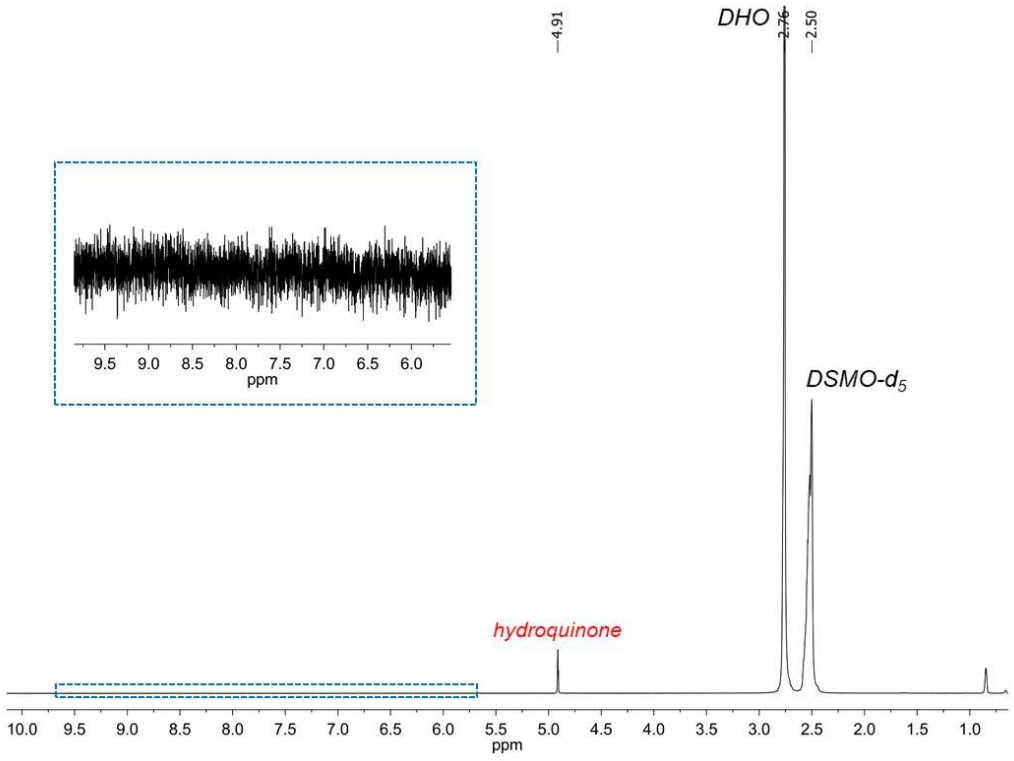

Figure S4. ^{1}H NMR spectrum (400 MHz, D_2O) proving the absence of **CBPQT**$^{4+}$ in solution after a storage period of 3 months.

Self-assembly of G4 ⊂ CBPQT^{4+}

Guest **G4** (1 equiv) was added to a solution of [**CBPQT**]Cl_4 in D_2O (2.5 mM). The resulting blue-colored solution was then analyzed by ^1H NMR spectroscopy (Figure S5b). A similar system was prepared in a mixture of ethanol/water (3/1, v/v) as the solvent, and analyzed by UV-vis spectroscopy (**Figure S6**).

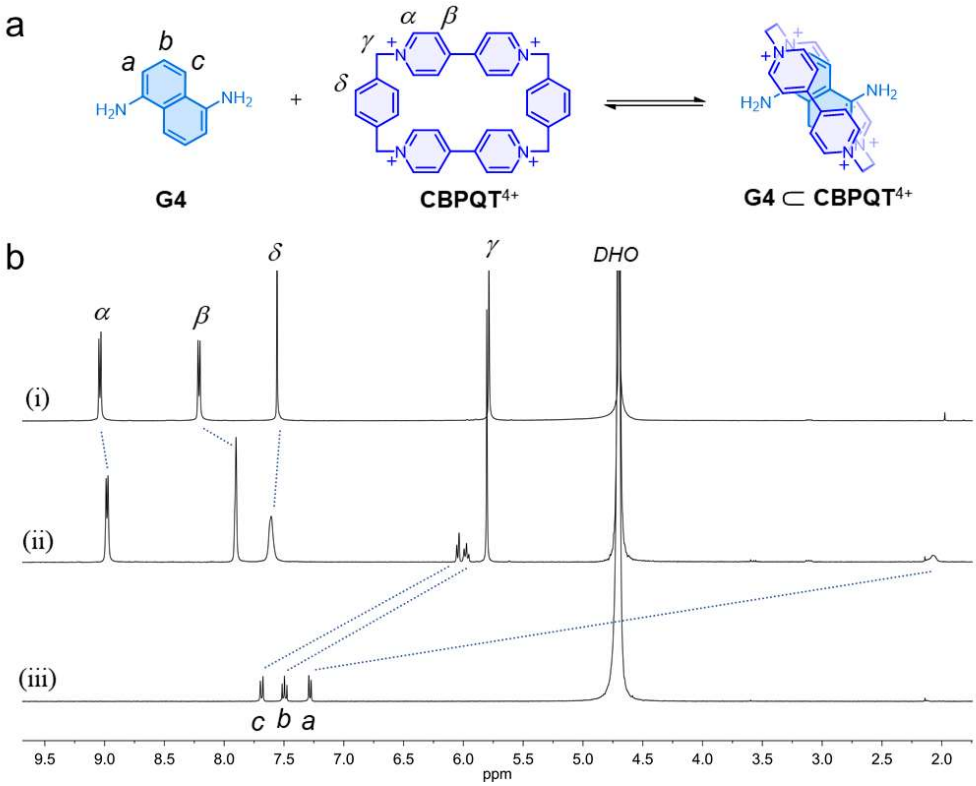

Figure S5. (a) Scheme for the self-assembly of complex **G4** ⊂ **CBPQT**$^{4+}$. (b) ^1H NMR spectra (400 MHz, D_2O) of (i) [**CBPQT**]Cl_4, (ii) an equimolar mixture of [**CBPQT**]Cl_4 and **G4**, and (iii) **G4**.

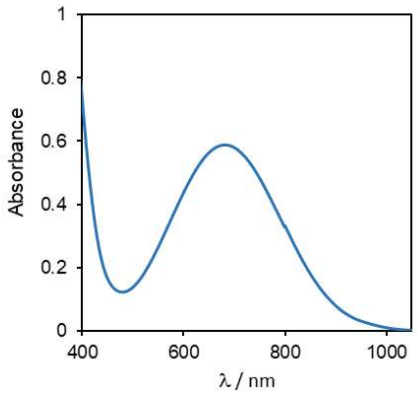

Figure S6. UV-vis spectrum of an equimolar mixture of [**CBPQT**]Cl_4 and **G4** prepared in ethanol/water (3/1, v/v).

UV-vis spectra of G4 ⊂ CBPQT^{4+}: solid state vs. solution

Figure S7 shows a comparison of the CT band of **G4 ⊂ CBPQT**$^{4+}$ detected in solution and in the solid state by UV-vis spectroscopy. Prior to analyzing the film, it was rinsed with ethanol/water (5 mL, 3/1, v/v).

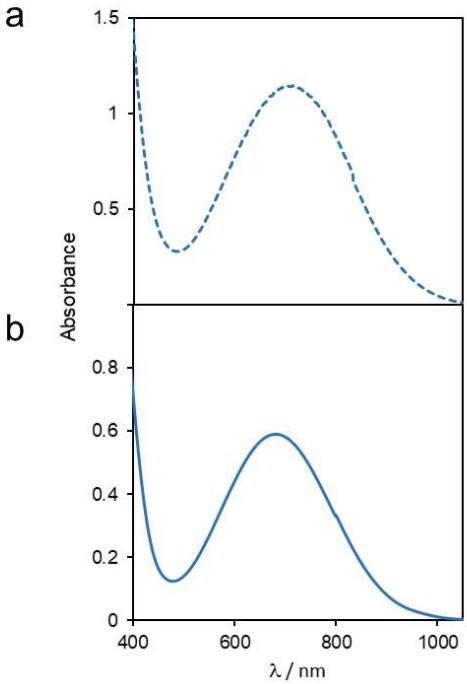

Figure S7. UV-vis spectra of complex **G4 ⊂ CBPQT**$^{4+}$; (a) in-film and (b) solution (prepared by mixing equimolar amounts of [**CBPQT**]Cl_4 and **G4** (2.5 mM) in ethanol/water (3/1, v/v)).

Controlling guest limiting uptake

Four different CNC-**CBPQT**$^{4+}$ films (ca. 15 mg) containing 1, 2, 3 and 7 wt% of host, were submerged in a solution of **G3** (50 mM, ethanol/water (3/1, v/v)) for 30 min at room temperature. The materials were then removed from solution and rinsed with ethanol/water (5 mL, 3/1, v/v) before analyzing them by UV-vis spectroscopy. The collected data are summarized in **Figure S8**.

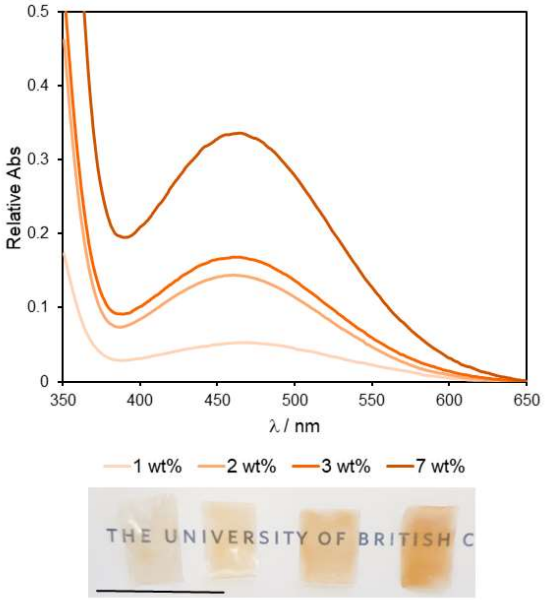

Figure S8. UV-vis spectra of the in-film complex **G3** ⊂ **CBPQT**$^{4+}$, formed within CNC-**CBPQT**$^{4+}$ matrices composed of 1, 2, 3, and 7 wt% of host (top). Photographs of the four assembled in-film complexes (bottom). Scale bar = 1 cm.

Testing a non-guest molecule

Molecule **M1** contains a π-electron-rich core (same as **G5**) that could interact with the host. It also features bulky groups at each end, however, that were expected to prevent intercomponent self-assembly. **Figure S9** shows the UV-vis spectra of a CNC-**CBPQT**$^{4+}$ film (3 wt% host) before and after been submerged in a solution of **M1** for 2 h (10 mM, ethanol/water (3/1, v/v)). There was no evidence, neither spectroscopic nor macroscopic, of in-film self-assembly.

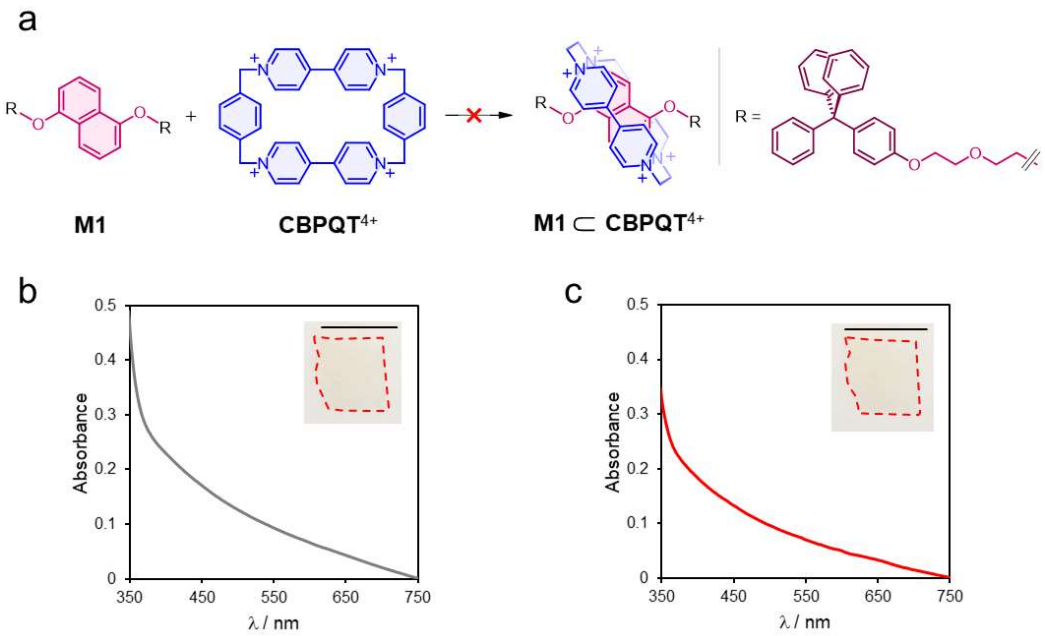

Figure S9. (a) Attempted assembly of **M1** ⊂ **CBPQT**$^{4+}$. UV-vis spectra of a CNC-**CBPQT**$^{4+}$ film (3 wt% host) (b) before and (c) after been exposed to a solution of **M1** (10 mM, ethanol/water (3/1, v/v)) for 2 h at room temperature. The inset pictures show the analyzed materials. Scale bars = 1 cm.

Acid-triggered disassembly of in-film G4 ⊂ CBPQT^{4+}

A solution of HCl (5 mL, 50 mM), prepared in ethanol/water (3/1, v/v), was added to the in-film complex **G4 ⊂ CBPQT**$^{4+}$ (total mass of ca. 15 mg). After storing for 1 h at room temperature, the film was removed and washed with ethanol/water (10 mL, 3/1, v/v). The recovered acid solution was evaporated, and the residue was analyzed by ^{1}H NMR spectroscopy in D_2O. The result is shown in **Figure S10**.

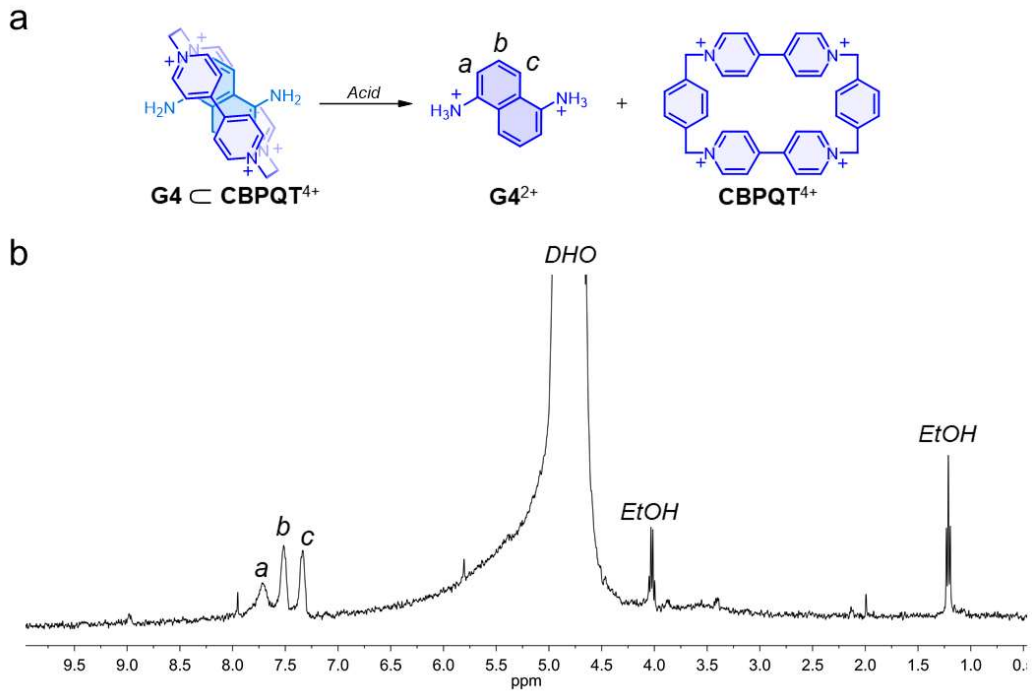

Figure S10. ^{1}H NMR spectrum (400 MHz, D_2O) of **G4**$^{2+}$, released after guest protonation.

The in-film complex **G6 ⊂ CBPQT**$^{4+}$ was disassembled under the same conditions.

Heat-triggered disassembly of in-film G5 ⊂ CBPQT^{4+}

A CNC-**CBPQT**$^{4+}$ film (ca. 8 mg) containing complex **G5** ⊂ **CBPQT**$^{4+}$ was submerged in ethanol/water (5 mL, 3/1, v/v) and heated at 70 ºC until it changed from purple to colorless (ca. 2.5 h). After removing the film from solution (while hot), it was rinsed with ethanol/water (10 mL, 3/1, v/v). The combined solutions were dried under vacuum and the residue was analyzed by ^{1}H NMR spectroscopy (see **Figure S11**).

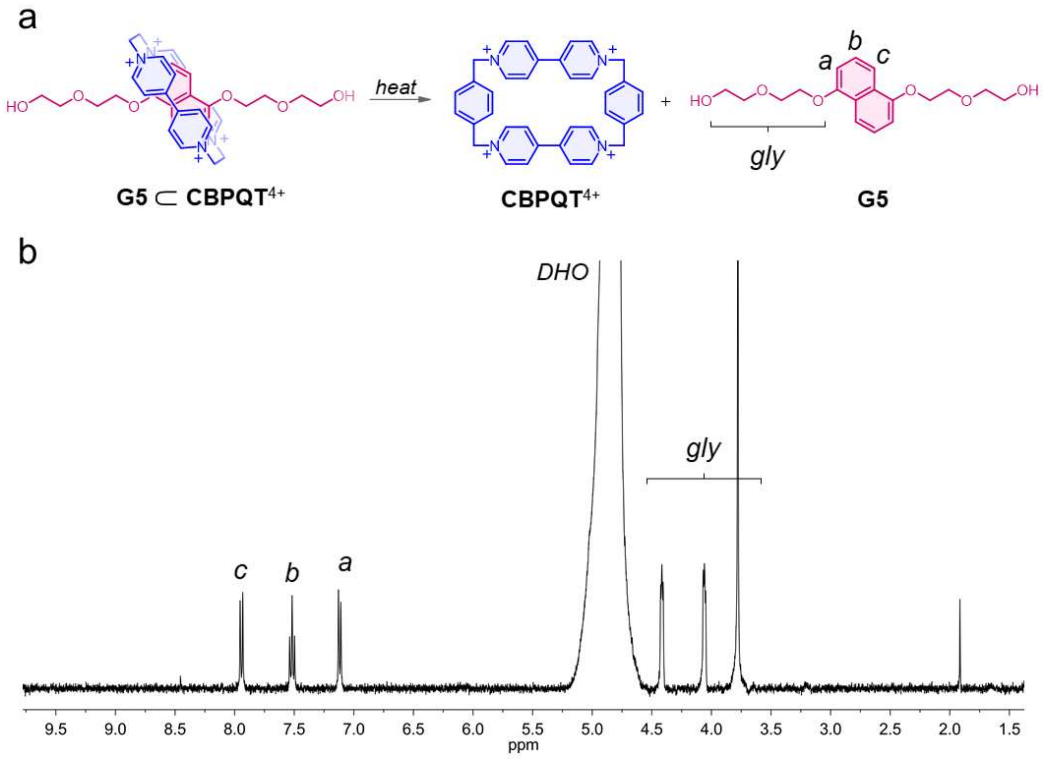

Figure S11. (a) Scheme of the heat-driven disassembly of in-film **G5** ⊂ **CBPQT**$^{4+}$. (b) ^{1}H NMR spectrum (400 MHz, D_2O) of the released guest **G5**.

Following the same protocol, the in-film complexes **G1** ⊂ **CBPQT**$^{4+}$, **G2** ⊂ **CBPQT**$^{4+}$ and **G3** ⊂ **CBPQT**$^{4+}$ were disassembled.

In-film guest exchange

Tracking by reflectance spectroscopy

A CNC-**CBPQT**$^{4+}$ film (ca. 12 mg, 3 wt% host) was submerged in a solution of **G1** (2 mL, 50 mM, ethanol/water (3/1, v/v)) and monitored *in-situ* for 2 h at room temperature using a submergible UV-vis reflection probe. After the analysis, the solution of **G1** was removed, followed by the rinsing of the film with ethanol/water (5 mL, 3/1, v/v). The film was then submerged in the next guest solution (50 mM, ethanol/water (3/1, v/v) and monitored as described before. We analyzed the exchange process in the following order: **G1** → **G2** → **G3** → **G4** → **G5** → **G6**. **Figure S12** shows a representative photograph of the employed setup and a summary of the collected data.

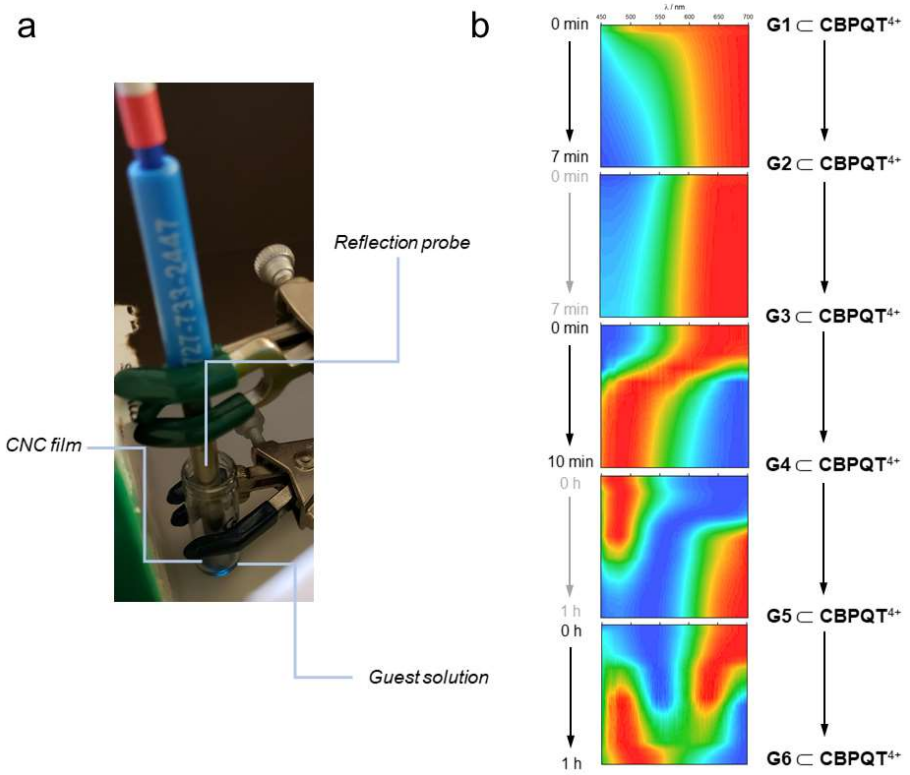

Figure S12. (a) Setup employed for the monitoring of in-film guest exchange. (b) Time-resolved reflectance spectra corresponding to the exchange process. The color scale goes from blue (minimum) to red (maximum); each 1-D spectrum was individually normalized prior to building the 2-D plots to emphasize the shift in reflectance maxima.

Inverse guest exchange

A CNC-**CBPQT**$^{4+}$ film (ca. 10 mg, 3 wt% host) was immersed in a solution of **G6** (2 mL, 50 mM, ethanol/water (3/1, v/v)) for 30 min and monitored macroscopically at room temperature (these conditions were employed to obtained the films shown in **Figure S13**a, which represent guest exchange **G2 → G3 → G4 → G5 → G6**). The solution of **G6** was removed and the film was rinsed with ethanol/water (5 mL, 3/1, v/v). We then submerged the obtained material in the next guest solution (50 mM, ethanol/water (3/1, v/v), 30 min). The exchange process was tested in the following order: **G6 → G5 → G4 → G3 → G2**; our observations are depicted in **Figure S13**b. The red outlines highlight two steps where guest exchange failed.

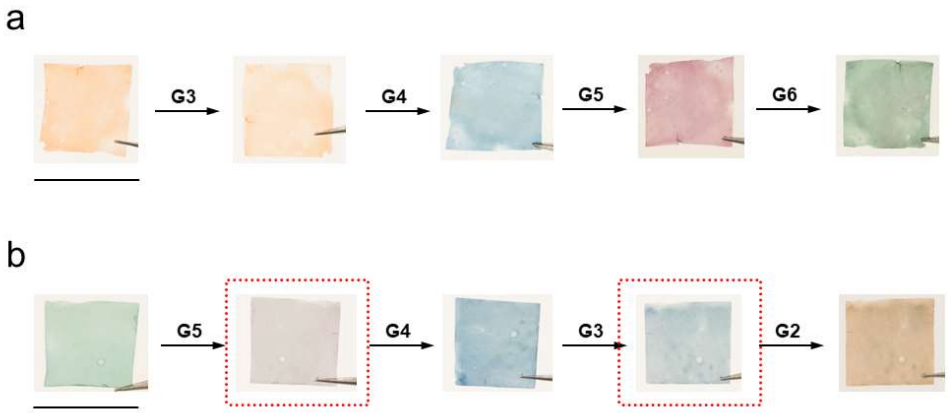

Figure S13. Photographs of the films obtained by guest exchange. Exchange guided by (a) increasing affinity **G2 → G6**, and (b) decreasing affinity **G6 → G2**. Scale bars = 1 cm.

Preparation of G5/G6 dynamic ink

G5 (0.66 equiv) and **G6** (0.33 equiv) were added to a solution of [**CBPQT**]Cl_4 (2.5 mM) prepared in ethanol/water (3/1, v/v). The resulting violet-colored solution was then analyzed by UV-vis spectroscopy before and after the addition of two equivalents (relative to **G6**) of a HCl solution (50 mM, ethanol/water (3/1, v/v)), see Figure S14b.

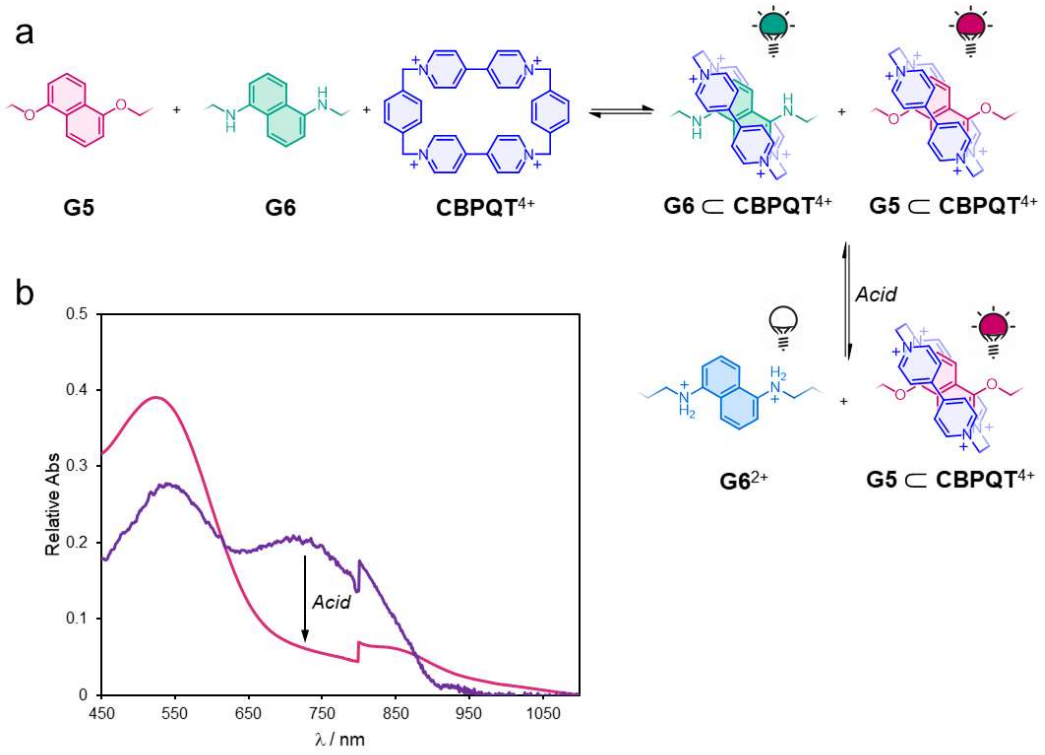

Figure S14. (a) Scheme for the formulation of a dynamic ink composed of **G5** and **G6**. (b) UV-vis spectra of a mixture of **G5** (0.66 equiv), **G6** (0.33 equiv) and [**CBPQT**]Cl_4 (2.5 mM) prepared in ethanol/water (3/1, v/v); CT bands before (violet) and after (purple) the addition of acid (2 equiv with respect to **G6**).

An analogous sample was prepared in D_2O and analyzed by ^1H NMR spectroscopy. In the collected spectrum (**Figure S15**), we confirmed the coexistence of **G5** ⊂ **CBPQT**$^{4+}$ and **G6** ⊂ **CBPQT**$^{4+}$, whereas upon the addition of acid, only **G5** ⊂ **CBPQT**$^{4+}$ remained assembled.

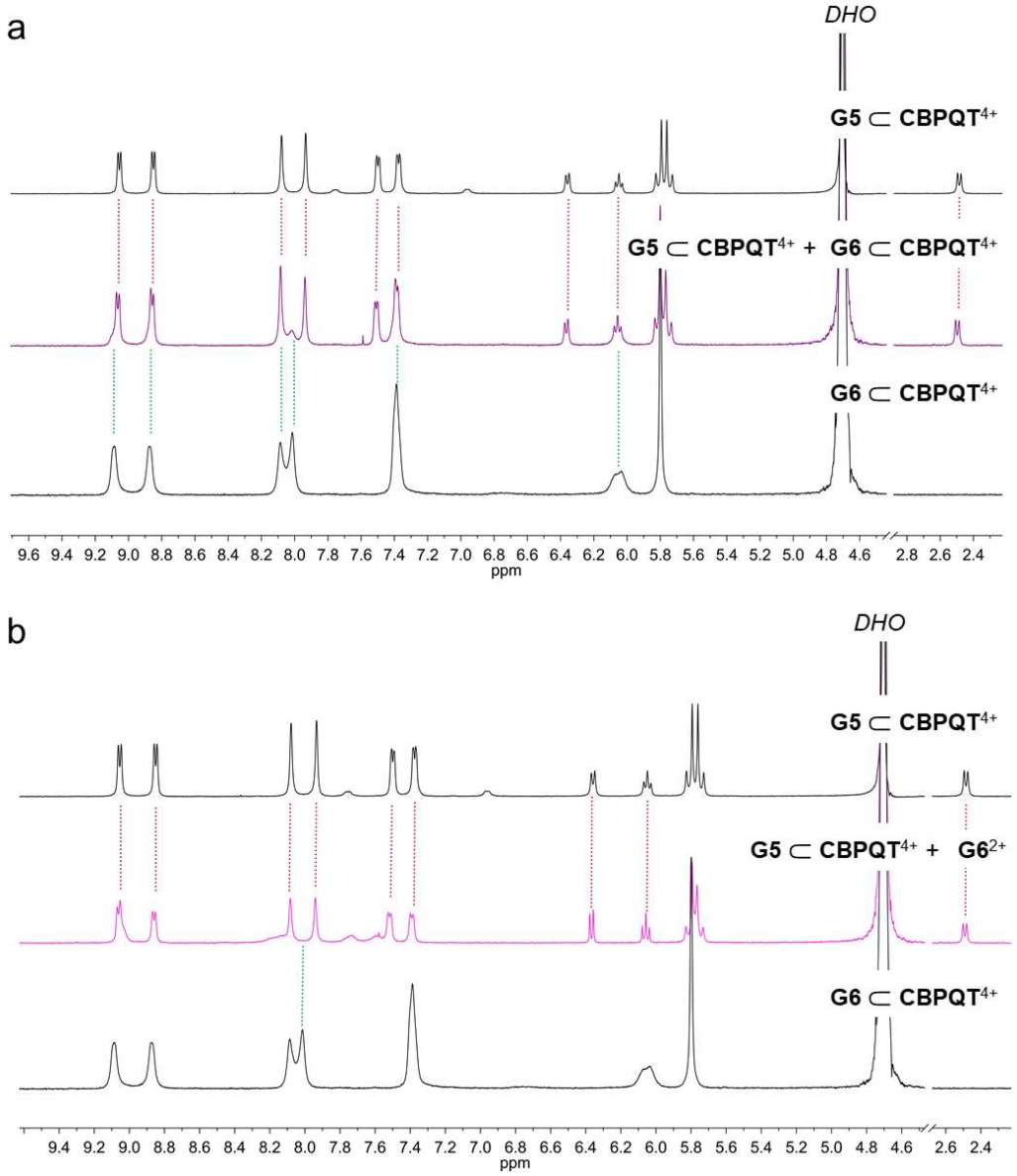

Figure S15. ^1H NMR spectra (400 MHz, D_2O) of a sample containing **G5** (0.66 equiv), **G6** (0.33 equiv) and [**CBPQT**]Cl_4 (2.5 mM); (a) before (violet) and (b) after (purple) the addition of acid (2 equiv relative to **G6**). Both (a) and (b) sets contain individual spectra of complexes **G5** ⊂ **CBPQT**$^{4+}$ (top) and **G6** ⊂ **CBPQT**$^{4+}$ (bottom) as references.

In-solution self-assembly of host–guest complexes

The self-assembly of the inclusion complexes **G1** ⊂ **CBPQT**$^{4+}$, **G2** ⊂ **CBPQT**$^{4+}$, **G3** ⊂ **CBPQT**$^{4+}$, **G4** ⊂ **CBPQT**$^{4+}$, **G5** ⊂ **CBPQT**$^{4+}$, and **G6** ⊂ **CBPQT**$^{4+}$ was studied by ^{1}H NMR (D_2O) and UV-vis spectroscopy (ethanol/water, 3/1, v/v). The corresponding guest molecule was added (1 equiv) to a solution of [**CBPQT**]Cl_4 (2.5 mM) and analyzed by the respective technique. Figure S16 to Figure S21 show the collected results.

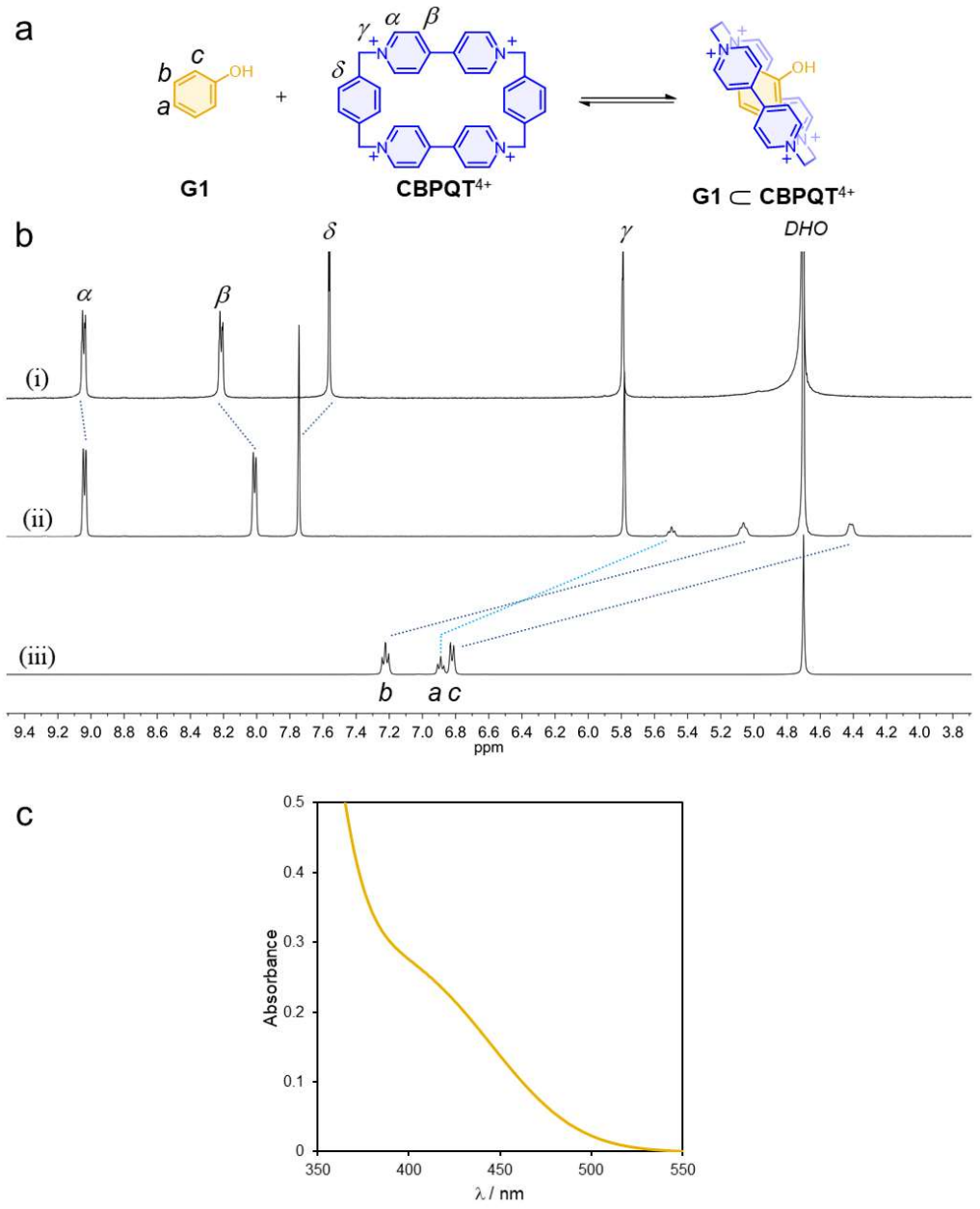

Figure S16. (a) Scheme for the self-assembly of complex **G1** ⊂ **CBPQT**$^{4+}$. (b) ^{1}H NMR spectra (400 MHz, D_2O) of (i) [**CBPQT**]Cl_4, (ii) an equimolar mixture of [**CBPQT**]Cl_4 and **G1**, and (iii) **G1**. (c) UV-vis spectrum of an equimolar mixture of [**CBPQT**]Cl_4 and **G1** prepared in ethanol/water (3/1, v/v).

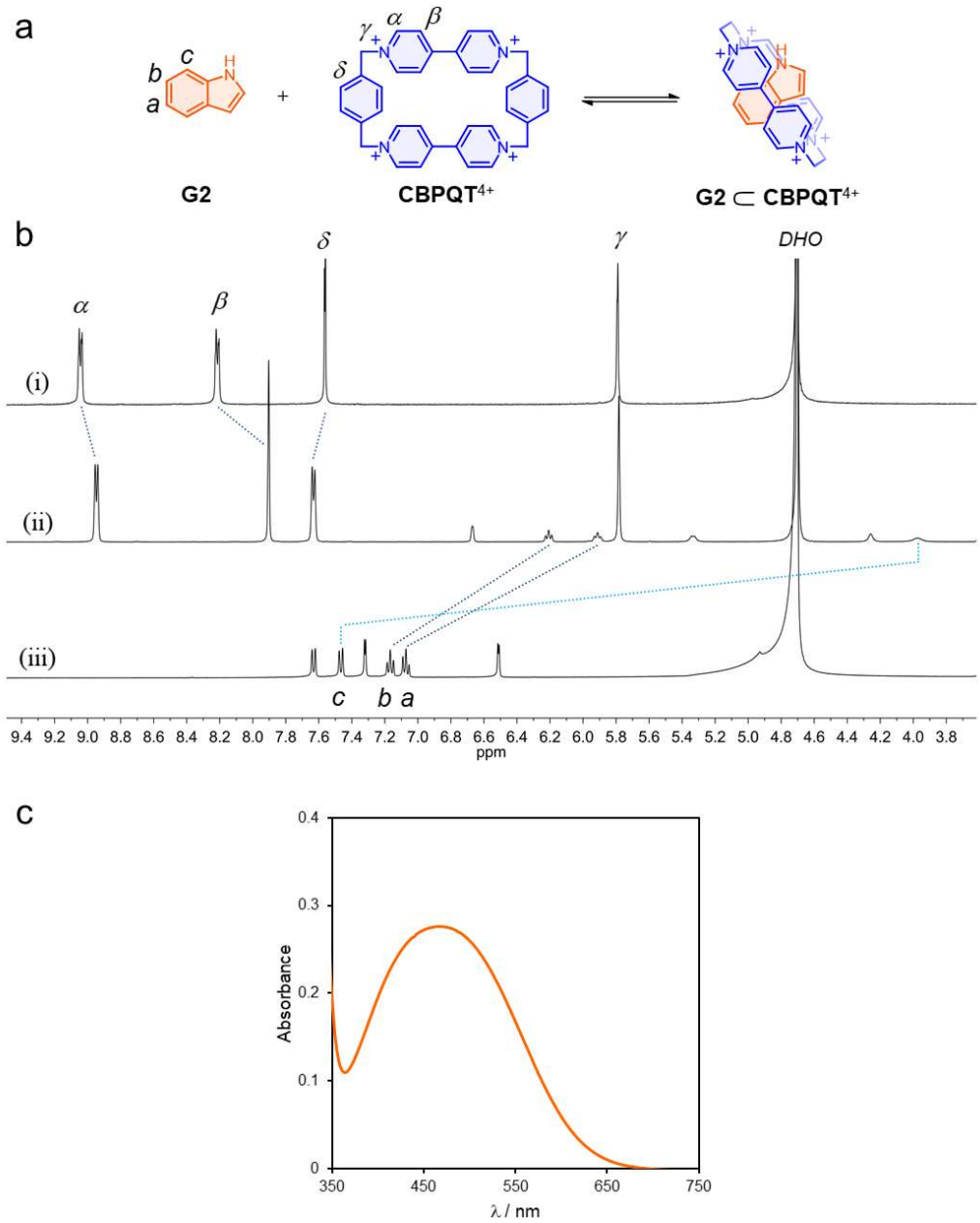

Figure S17. (a) Scheme for the self-assembly of **G2** ⊂ **CBPQT**$^{4+}$. (b) ^{1}H NMR spectra (400 MHz, D_2O) of (i) [**CBPQT**]Cl_4, (ii) an equimolar mixture of [**CBPQT**]Cl_4 and **G2**, and (iii) **G2**. (c) UV-vis spectrum of an equimolar mixture of [**CBPQT**]Cl_4 and **G2** prepared in ethanol/water (3/1, v/v).

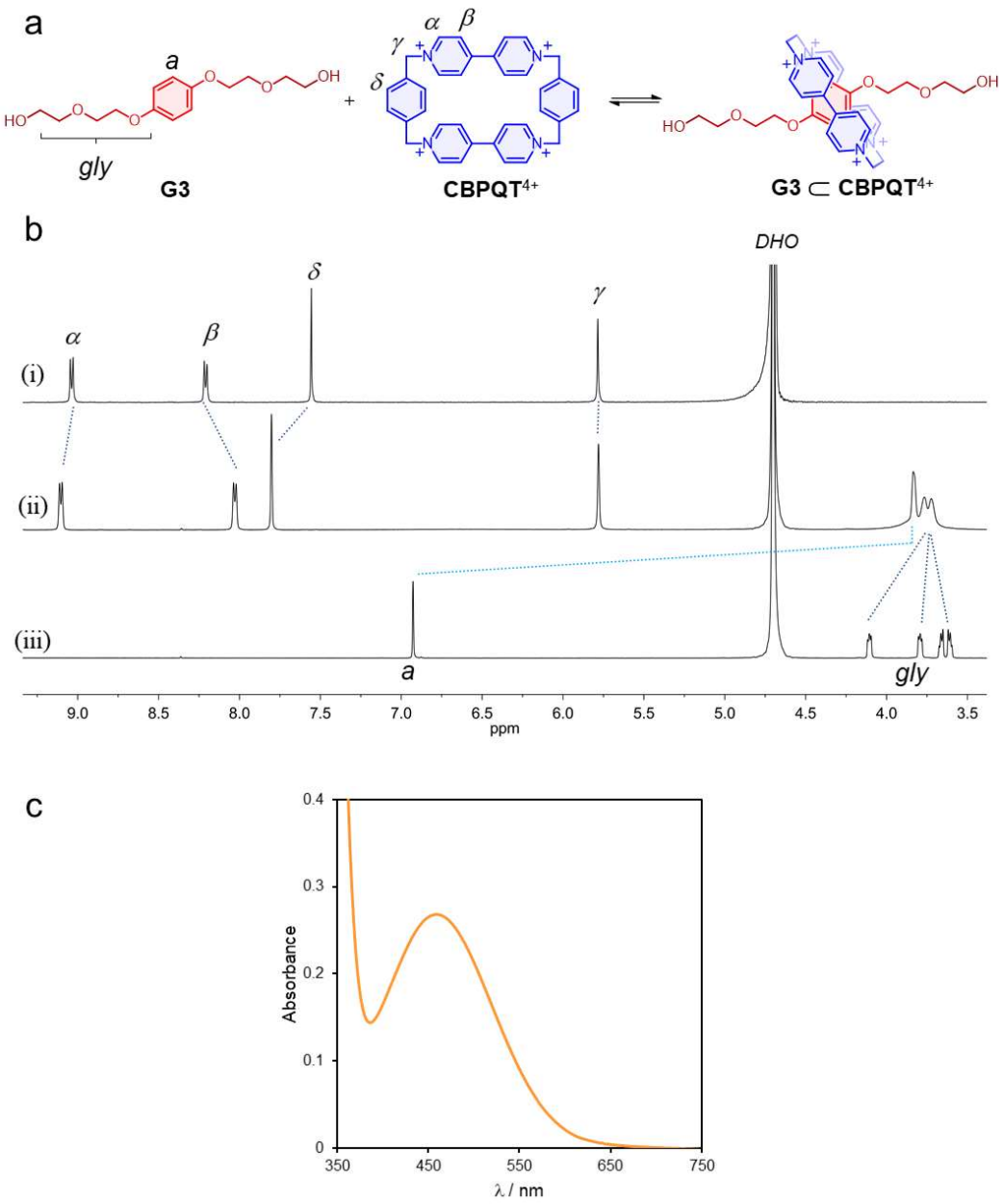

Figure S18. (a) Scheme for the self-assembly of complex **G3** ⊂ **CBPQT**$^{4+}$. (b) ^{1}H NMR spectra (400 MHz, D_2O) of (i) [**CBPQT**]Cl_4, (ii) an equimolar mixture of [**CBPQT**]Cl_4 and **G3**, and (iii) **G3**. (c) UV-vis spectrum of an equimolar mixture of [**CBPQT**]Cl_4 and **G3** prepared in ethanol/water (3/1, v/v).

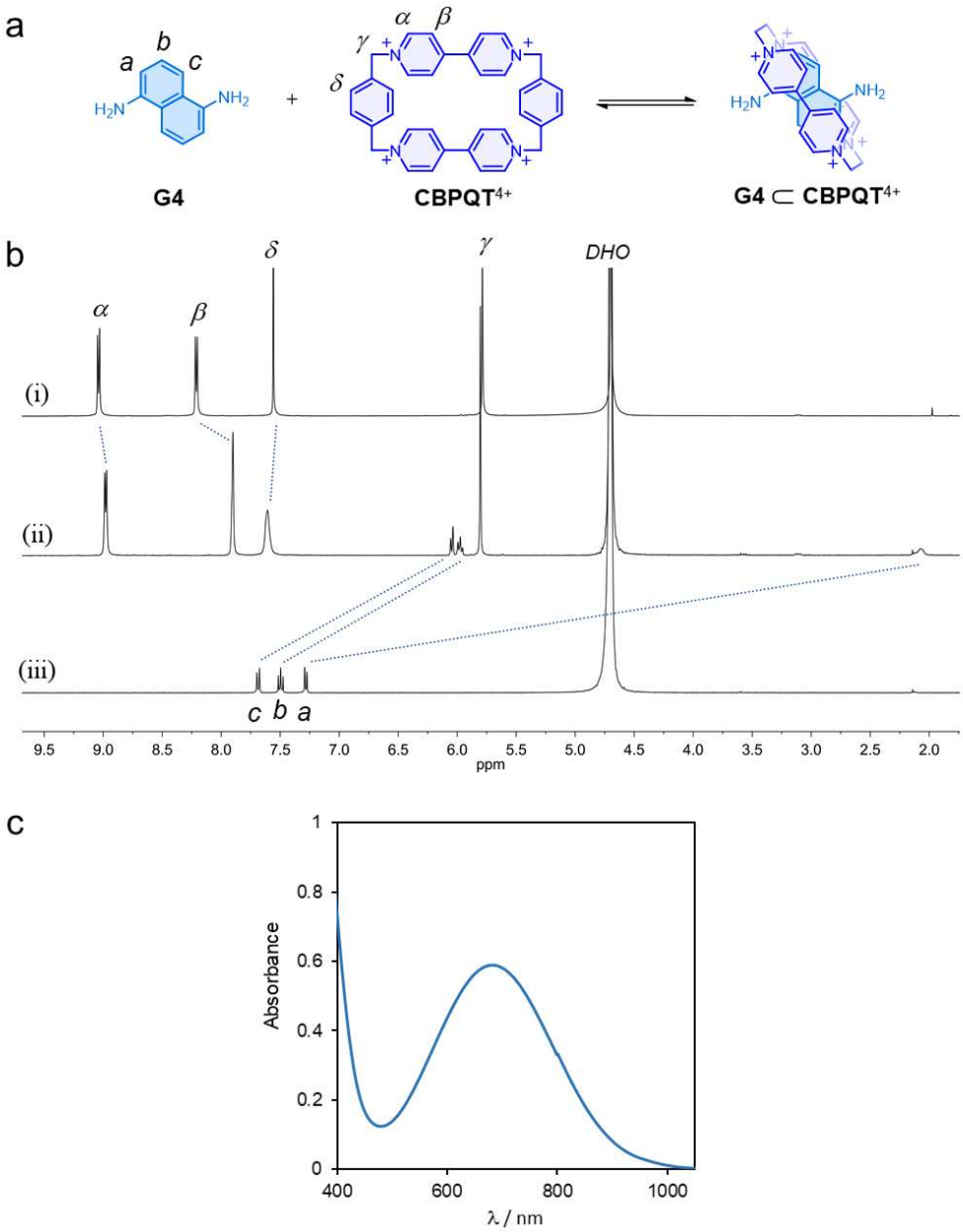

Figure S19. (a) Scheme for the self-assembly of complex **G4** ⊂ **CBPQT**$^{4+}$. (b) ^{1}H NMR spectra (400 MHz, D_2O) of (i) [**CBPQT**]Cl_4, (ii) an equimolar mixture of [**CBPQT**]Cl_4 and **G4**, and (iii) **G4**. (c) UV-vis spectrum of an equimolar mixture of [**CBPQT**]Cl_4 and **G4** prepared in ethanol/water (3/1, v/v).

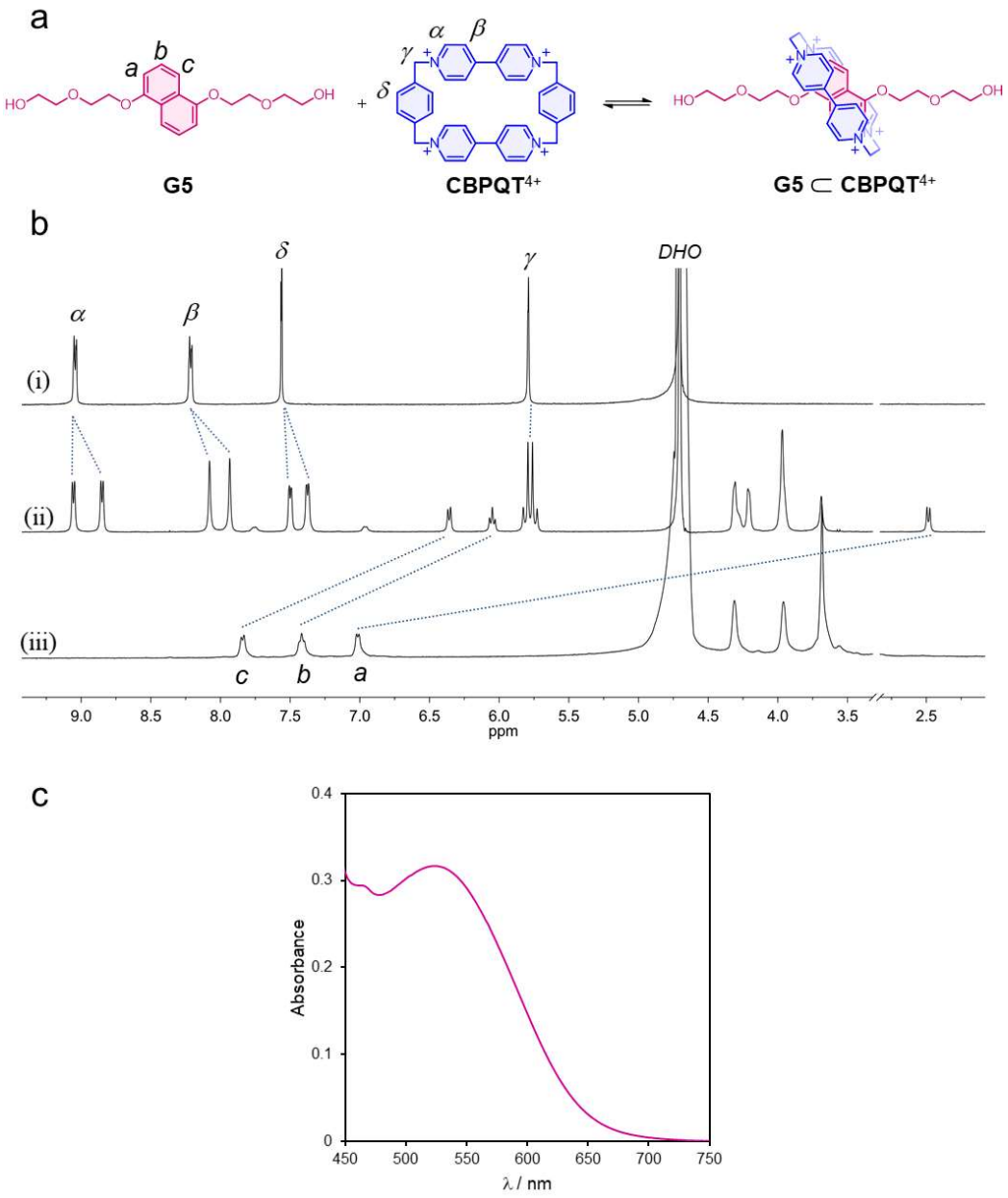

Figure S20. (a) Scheme for the self-assembly of complex **G5** ⊂ **CBPQT**$^{4+}$. (b) ^{1}H NMR spectra (400 MHz, D_2O) of (i) [**CBPQT**]Cl_4, (ii) an equimolar mixture of [**CBPQT**]Cl_4 and **G5**, and (iii) **G5**. (c) UV-vis spectrum of an equimolar mixture of [**CBPQT**]Cl_4 and **G5** prepared in ethanol/water (3/1, v/v).

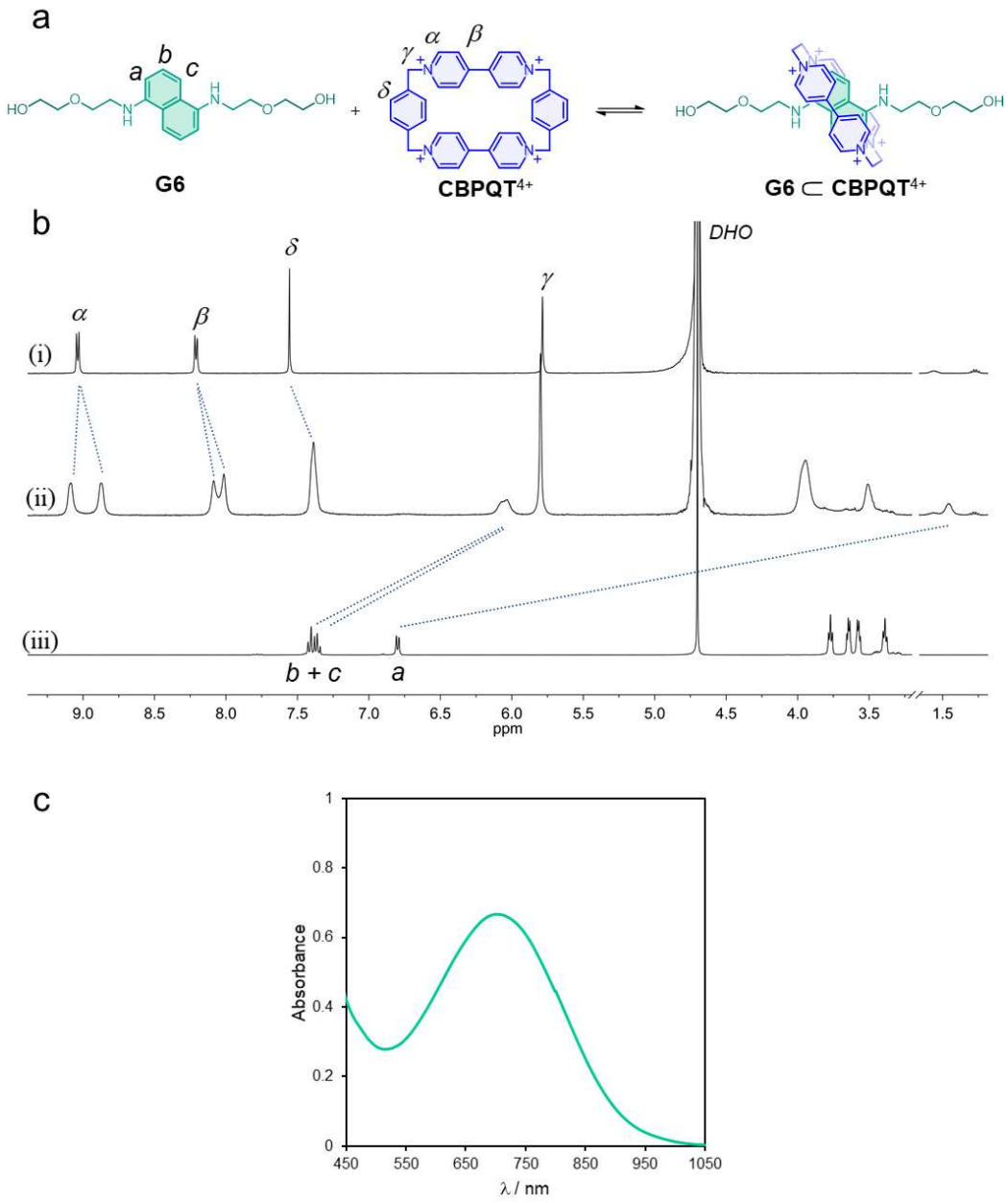

Figure S21. (a) Scheme for the self-assembly of complex **G6** ⊂ **CBPQT**$^{4+}$. (b) ^{1}H NMR spectra (400 MHz, D_2O) of (i) [**CBPQT**]Cl_4, (ii) an equimolar mixture of [**CBPQT**]Cl_4 and **G6**, and (iii) **G6**. (c) UV-vis spectrum of an equimolar mixture of [**CBPQT**]Cl_4 and **G6** prepared in ethanol/water (3/1, v/v).

Binding affinity analyses

The stability constants (K_a) of **G1** ⊂ **CBPQT**$^{4+}$, **G2** ⊂ **CBPQT**$^{4+}$, **G3** ⊂ **CBPQT**$^{4+}$, **G4** ⊂ **CBPQT**$^{4+}$, **G5** ⊂ **CBPQT**$^{4+}$, and **G6** ⊂ **CBPQT**$^{4+}$ were determined by the titration of the host with the respective guests in ethanol/water (3/1, v/v, at 25 °C). Each experiment was performed in triplicate by UV-vis spectroscopy. Figure S22 to Figure S27 show representative data.

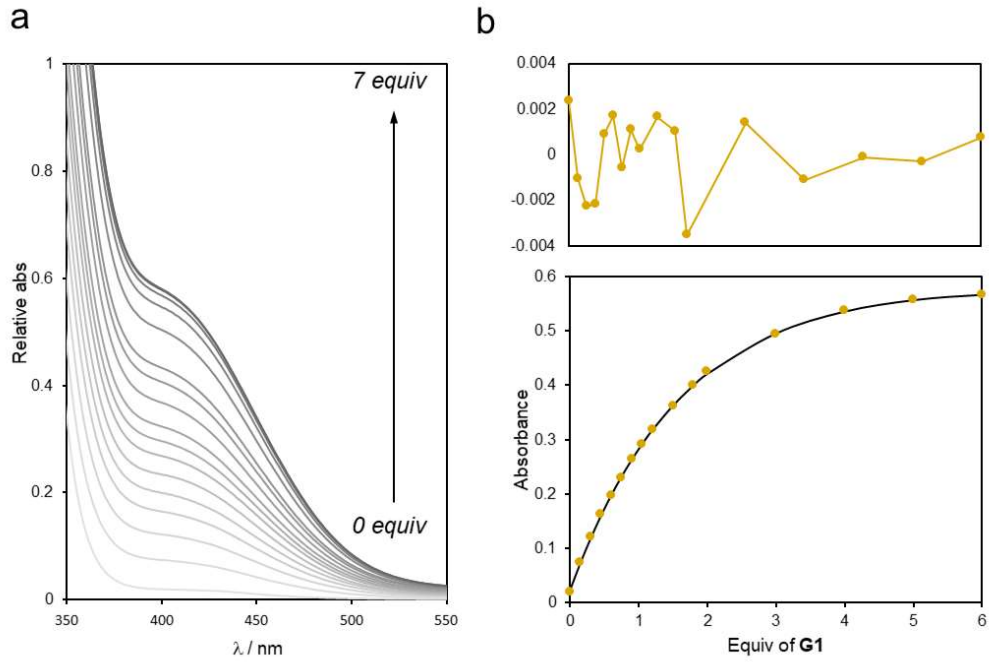

Figure S22. (a) UV-vis spectra resulting of the titration of a host solution (2 mM) with **G1** (50 mM) in ethanol/water (3/1, v/v, 25 ºC). (b) Titration isotherm (bottom) and residuals plot (top) derived from a non-linear least-squares fitting. Experimental data (yellow dots); fitting (black line).

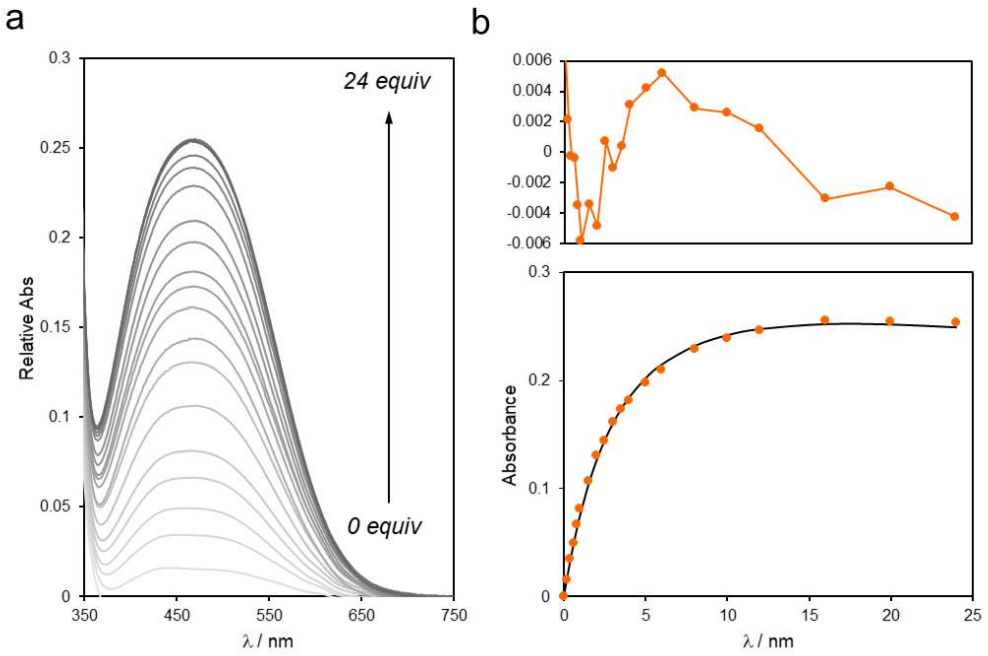

Figure S23. (a) UV-vis spectra resulting of the titration of a host solution (0.5 mM) with **G2** (50 mM) in ethanol/water (3/1, v/v, 25 ºC). (b) Titration isotherm (bottom) and residuals plot (top) derived from a non-linear least-squares fitting. Experimental data (orange dots); fitting (black line).

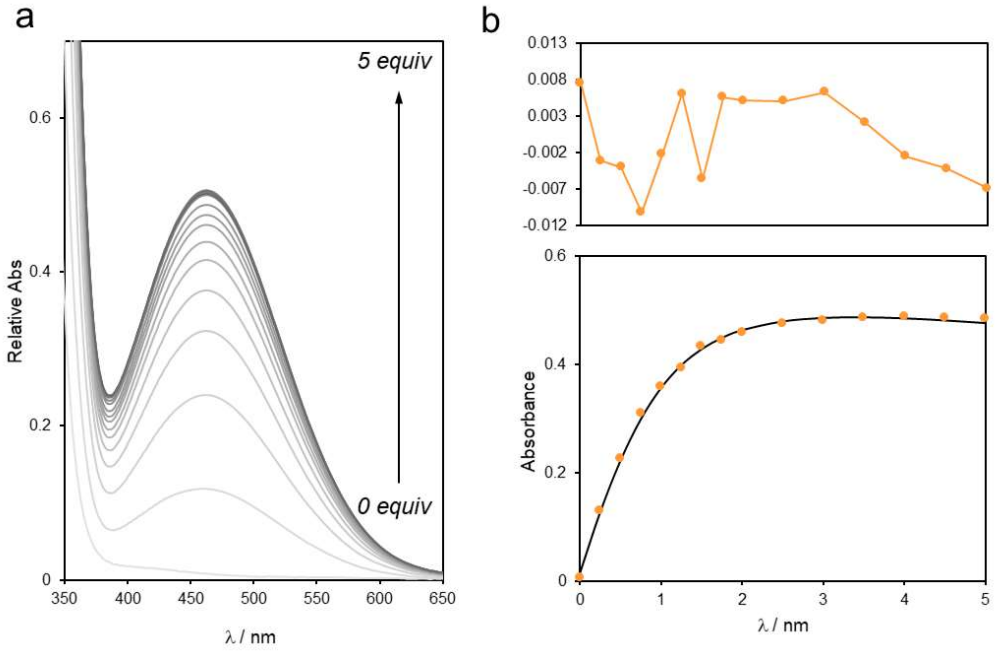

Figure S24. (a) UV-vis spectra resulting of the titration of a host solution (2.5 mM) with **G3** (50 mM) in ethanol/water (3/1, v/v, 25 ºC). (b) Titration isotherm (bottom) and residuals plot (top) derived from a non-linear least-squares fitting. Experimental data (orange dots); fitting (black line).

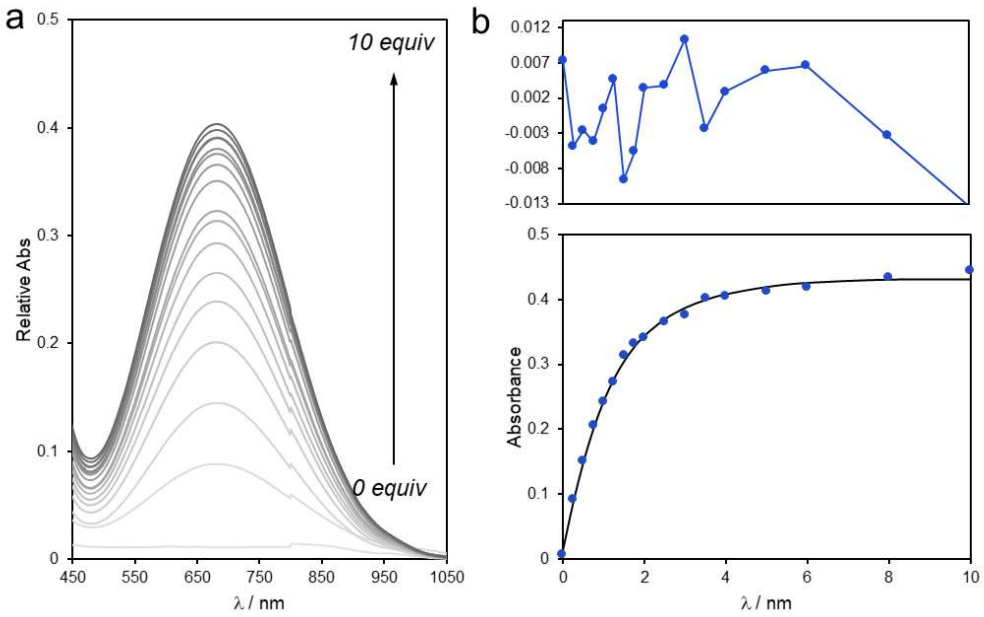

Figure S25. (a) UV-vis spectra resulting of the titration of a host solution (0.4 mM) with **G4** (50 mM) in ethanol/water (3/1, v/v, 25 ºC). (b) Titration isotherm (bottom) and residuals plot (top) derived from a non-linear least-squares fitting. Experimental data (blue dots); fitting (black line).

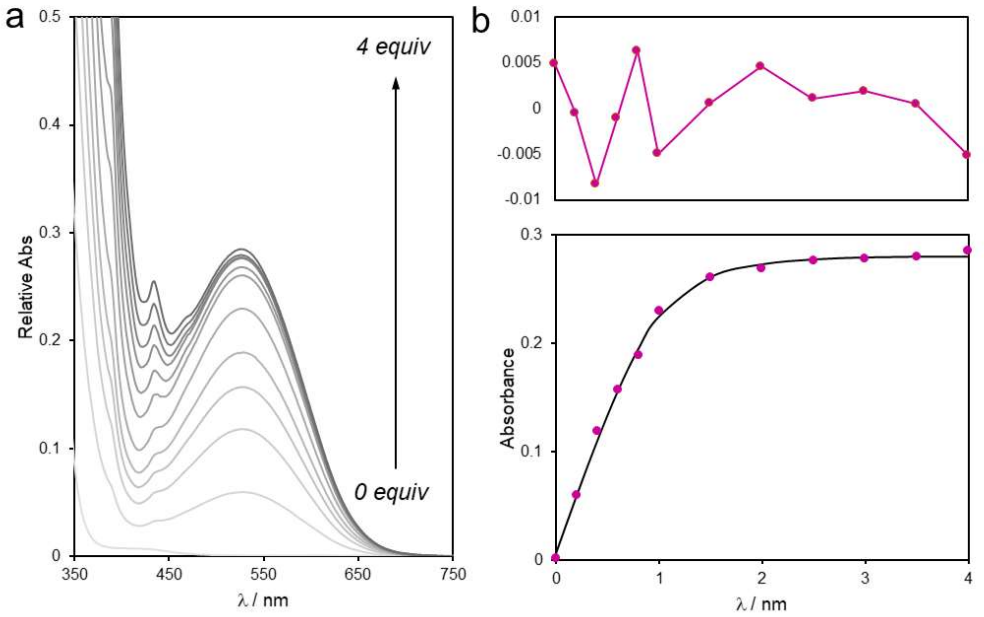

Figure S26. (a) UV-vis spectra resulting of the titration of a host solution (0.5 mM) with **G5** (25 mM) in ethanol/water (3/1, v/v, 25 ºC). (b) Titration isotherm (bottom) and residuals plot (top) derived from a non-linear least-squares fitting. Experimental data (purple dots); fitting (black line).

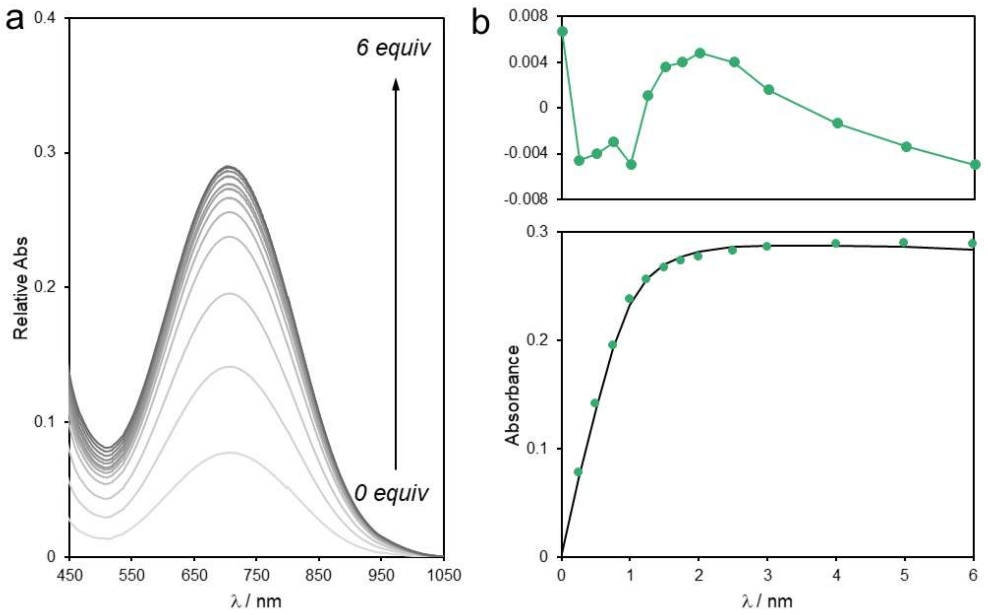

Figure S27. (a) UV-vis spectra resulting of the titration of a host solution (0.3 mM) with **G6** (25 mM) in ethanol/water (3/1, v/v, 25 ºC). (b) Titration isotherm (bottom) and residuals plot (top) derived from a non-linear least-squares fitting. Experimental data (green dots); fitting (black line).

The resulting isotherms were fitted by a non-linear least-squares method, employing the BindFit platform,[4] and utilizing a 1:1 global fitting model (Nelder-Mead method). The values obtained from this fitting are summarized in **Table S1**.

Table S1. Thermodynamic data corresponding to the self-assembly of host–guest complexes in ethanol/water (3/1, v/v) at 25 ºC, employing **CBPQT**$^{4+}$ as the host and **G**1–**G6** as guests.

Guest	K_a / M^{-1}	ΔG / kJ mol^{-1}
G1	277 ± 10	-13.9 ± 0.5
G2	713 ± 54	-16.3 ± 1.2
G3	1310 ± 80	-17.8 ± 1.1
G4	5235 ± 695	-21.2 ± 2.8
G5	30620 ± 7931	-25.6 ± 6.6
G6	42600 ± 2300	-26.4 ± 1.4

Standard deviations were estimated from three replicates.

In-film and solution CT bands

Figure S28 shows a comparison of the CT bands observed by UV-vis spectroscopy, both in solution and solid state, for each assembled host–guest complex.

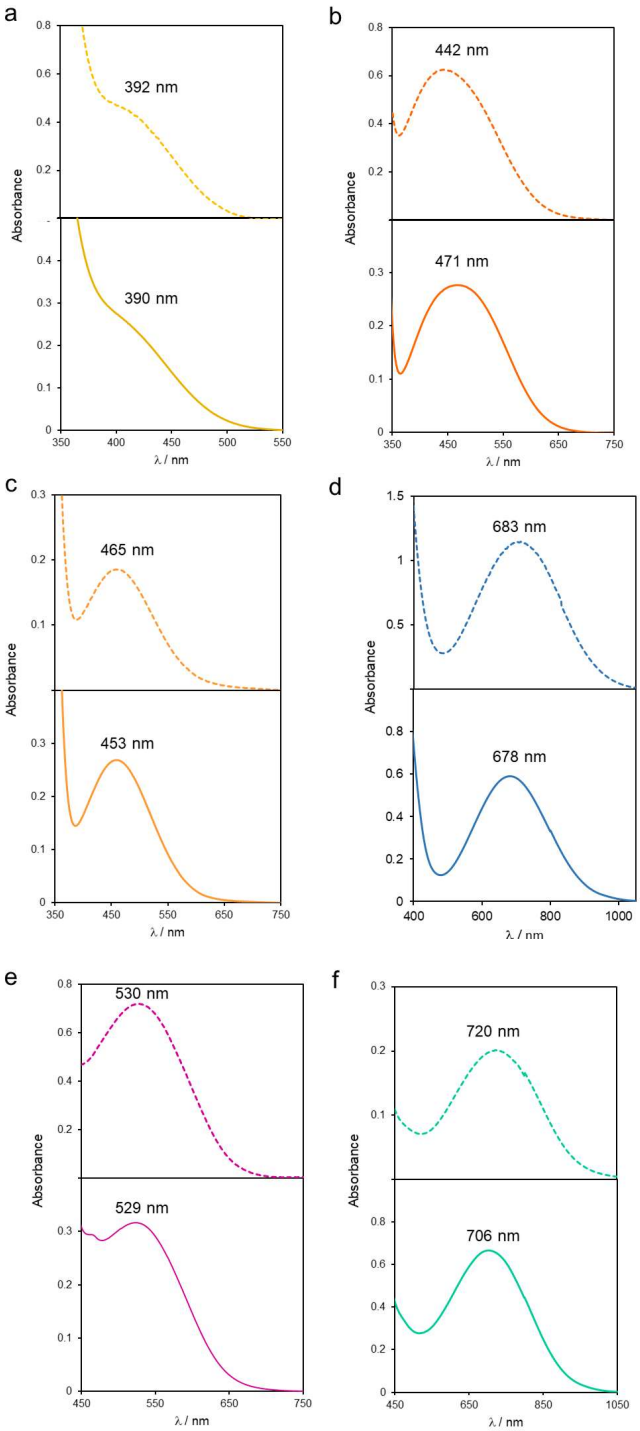

Figure S28. UV-vis spectra of the host–guest complexes prepared in solution (bottom) and within films (top), using (a) **G1**, (b) **G2**, (c) **G3**, (d) **G4**, (e) **G5**, and (f) **G6**.

X-Ray Characterization of [G4 ⊂ CBPQT]Cl_4

Experimental and data treatment

A green tablet-shaped crystal of [**G4** ⊂ **CBPQT**]Cl_4 (recrystallized from a mixture of ethanol/water 3/1, v/v, by slow evaporation) with dimensions 0.15 × 0.14 × 0.07 mm was mounted on a mylar loop in oil. Data were collected using a Bruker APEX II area detector diffractometer equipped with an Oxford Cryosystems low-temperature device operating at T = 90(2) K. Data were measured using ϕ and ω scans of 2.0° per frame for 20 and 90 s using CuK_α radiation (microfocus sealed X-ray tube, 45 kV, 0.60 mA). The total number of runs and images was based on the strategy calculation from the program APEX3. The maximum resolution that was achieved was Θ = 56.036° (0.93 Å). The unit cell was refined using SAINT[5] on 5953 reflections, 27% of the observed reflections. Data reduction, scaling and absorption corrections were performed using SAINT (Bruker, V8.40A, after 2013). The final completeness is 99.90 % out to 56.036° in Θ. A multi-scan absorption correction was performed using SADABS-2016/2 (Bruker, 2016/2). wR_2(int) was 0.1113 before and 0.0871 after correction. The ratio of minimum to maximum transmission is 0.7863. The λ/2 correction factor is not present. The absorption coefficient μ of this material is 2.719 mm^{-1} at this wavelength (λ = 1.54178Å) and the minimum and maximum transmissions are 0.650 and 0.827.

The structure was solved and the space group *Aea*2 (# 41) determined by the XT[6] structure solution program using Intrinsic Phasing methods (Olex2 graphical interface[7]) and refined by full matrix least squares minimisation on F^2 using version 2018/3 of XL.[8] This structure contains a layer of disordered chloride and water molecules. While the two can be nearly indistinguishable, the following strategy was employed to model this region as reasonably as possible. First, only the inclusion complex (both host and guest) were modeled, then the PLATON/SQUEEZE[9] program was used only to determine the amount of residual electron density in the lattice, the solvent-free data set was not used in subsequent refinements. According to SQUEEZE there were 787 unresolved electrons in the void space containing the chlorides and water. Space group Aea2 has 8 asymmetric units per unit cell, meaning there were 98.4 unmodeled electrons per asymmetric unit. In order to maintain charge balance, each asymmetric unit must have two chlorides, or 34 electrons, with the remaining 64.4 electrons belonging to solvent water molecules. This means approximately 6.4 water molecules per asymmetric unit. Next, the residual electron density peaks were assigned as oxygen atoms and their occupancies were allowed to refine freely. Those with occupancies greater than 1.0 were reassigned as chloride atoms. There were 5 such sites. The SUMP command was employed on these chlorides to restrict the sum of their occupancies to 2.0. Any remaining electron density peaks large enough to be modeled were assigned as oxygen atoms and the same strategy was employed, this time with the sum of all occupancies set to 6.4. Subsequently, in regions with overlapping fragments of chlorides and oxygens an additional SUMP command was used to ensure that the sum

of the occupancies at these sites would not greatly exceed 1.0. No hydrogen atoms were affixed to the oxygen atoms as their positions could not be determined with any certainty. All non-hydrogen atoms were refined anisotropically. Hydrogen atom positions were calculated geometrically and refined using the riding model. Amino hydrogen atoms were placed in calculated positions. In this case both nitrogen atoms had three hydrogens affixed, with one removed from each. The ones that were removed were the ones that generated the largest negative electron density.

The value of Z' is 0.5. This means that only half of the formula unit is present in the asymmetric unit, with the other half consisting of symmetry equivalent atoms. The Flack parameter was refined to 0.49(3). Determination of absolute structure using Bayesian statistics on Bijvoet differences using the Olex2 results in 0.50(2).[10] Note: The Flack parameter is used to determine chirality of the crystal studied, the value should be near 0, a value of 1 means that the stereochemistry is wrong, and the model should be inverted. A value of 0.5 means that the crystal consists of a racemic mixture of the two enantiomers.

Crystal Data

$C_{46}H_{67.13}Cl_{3.98}N_6O_{12.56}$, M_r = 1046.18, orthorhombic, *Aea*2 (No. 41), a = 17.9309(6) Å, b = 15.6796(6) Å, c = 17.7173(6) Å, $\alpha = \beta = \gamma = 90^\circ$, V = 4981.2(3) Å^3, T = 90(2) K, Z = 4, Z' = 0.5, μ(CuK$_\alpha$) = 2.719, 22142 reflections measured, 3175 unique (R_{int} = 0.0980) which were used in all calculations. The final wR_2 was 0.1837 (all data) and R_1 was 0.0666 (I > 2(I)).

Formula	$C_{46}H_{67.13}Cl_{3.98}N_6O_{12.56}$
$D_{calc.}$/ g cm^{-3}	1.395
μ/mm^{-1}	2.719
Formula Weight	1046.18
Colour	green
Shape	tablet
Size/mm^3	0.15×0.14×0.07
T/K	90(2)
Crystal System	orthorhombic
Flack Parameter	0.49(3)
Hooft Parameter	0.50(2)
Space Group	*Aea*2
a/Å	17.9309(6)
b/Å	15.6796(6)
c/Å	17.7173(6)
α/°	90
β/°	90
γ/°	90
V/Å^3	4981.2(3)
Z	4
Z'	0.5
Wavelength/Å	1.54178
Radiation type	CuK$_\alpha$
Θ_{min}/°	4.501
Θ_{max}/°	56.036
Measured Refl's.	22142
Ind't Refl's	3175
Refl's with I > 2(I)	2432
R_{int}	0.0980
Parameters	413

Restraints	549
Largest Peak	0.254
Deepest Hole	-0.257
GooF	1.069
wR_2 (all data)	0.1837
wR_2	0.1656
R_1 (all data)	0.0921
R_1	0.0666

Structure Quality Indicators

Reflections:

Refinement:

Packing images

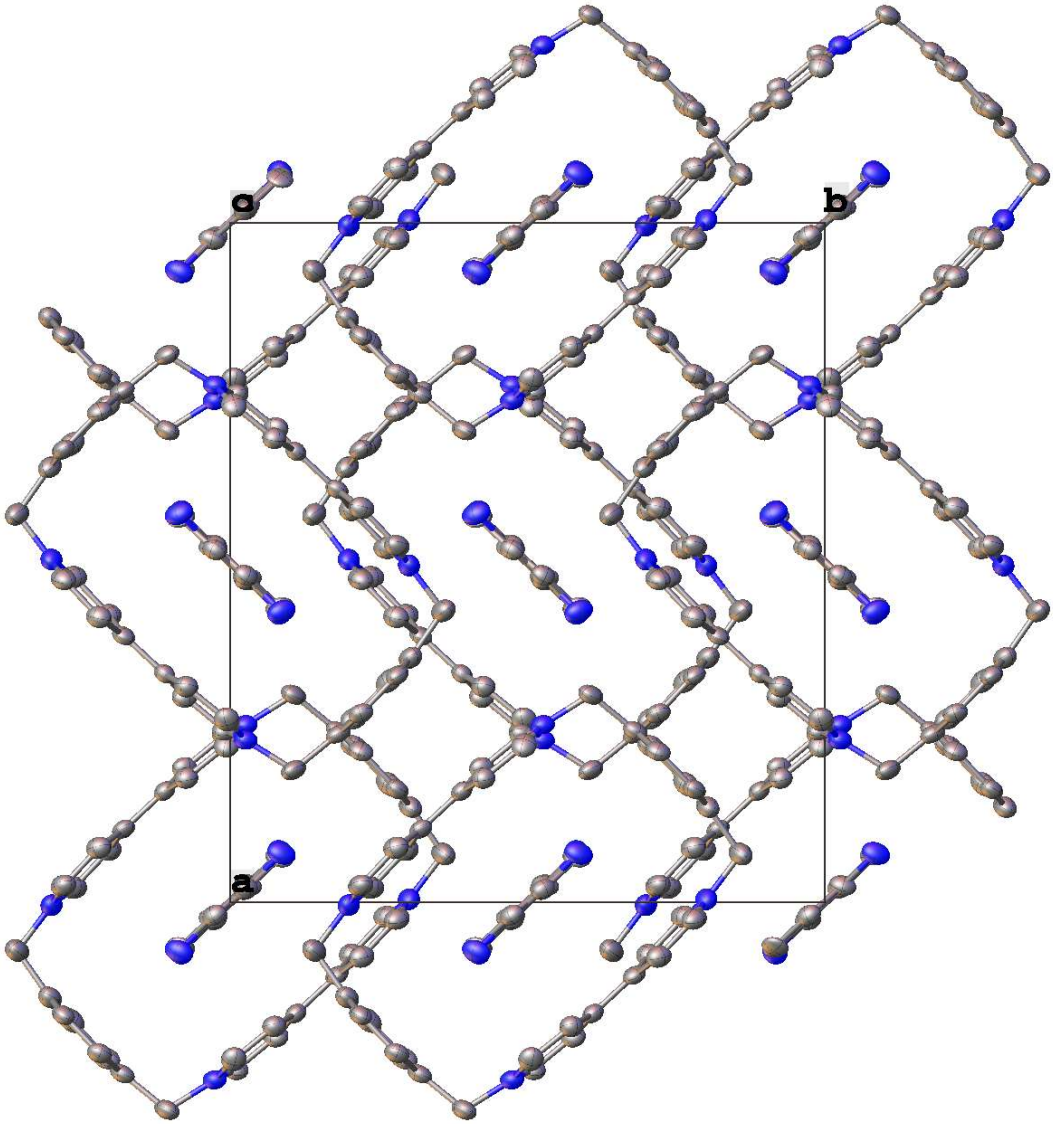

Figure S29. ORTEP-style picture of the packing, with the solvent/anion regions and hydrogen atoms removed, for clarity.

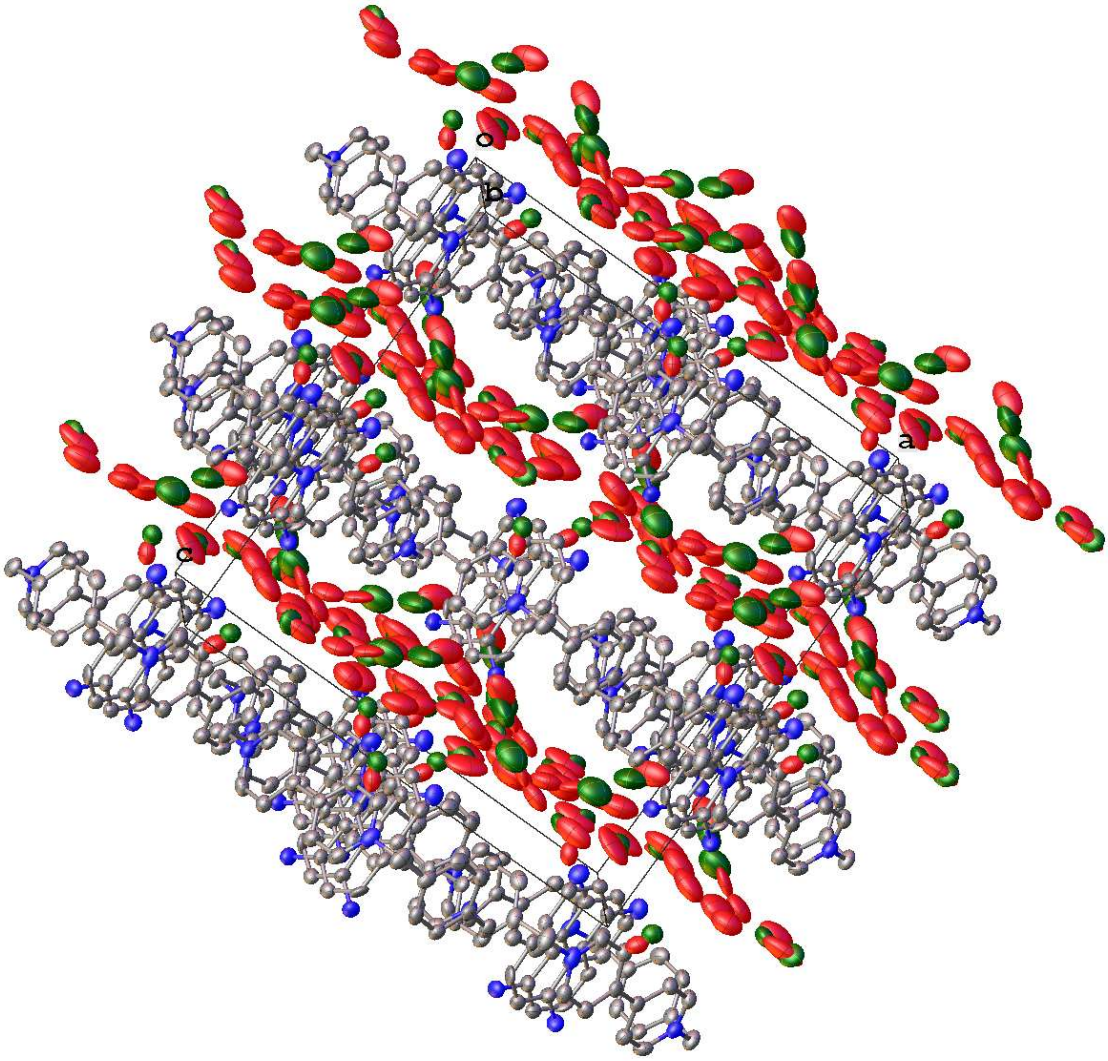

Figure S30. ORTEP-style picture of the packing with the solvent/anion layers shown.

References

1. W. Y. Hamad and T. Q. Hu, *Can. J. Chem. Eng.,* 2010, **88**, 392.

2. P. L. Anelli, P. R. Ashton, R. Ballardini, V. Balzani, M. Delgado, M. T. Gandolfi, T. T. Goodnow, A. E. Kaifer, D. Philp, M. Pietraszkiewicz, L. Prodi, M. V. Reddington, A. M. Z. Slawin, N. Spencer, J. F. Stoddart, C. Vicent and D. J. Williams, *J. Am. Chem. Soc.,* 1992, **114**, 193.

3. C. H. Sue, S. Basu, A. C. Fahrenbach, A. K. Shveyd, S. K. Dey, Y. Y. Botrosacd and J. F. Stoddart, *Chem. Sci.,* 2010, **1**, 119.

4. http://supramolecular.org | Accessed May 2020.

5. Software for the Integration of CCD Detector System Bruker Analytical X-ray Systems, Bruker AXS., Madison, WI (after 2013).

6. G. M. Sheldrick, *Acta Cryst.*, 2015, **A71**, 3.

7. O. V. Dolomanov, L. J. Bourhis, R. J. Gildea, J. A. K. Howard and H. Puschmann, *J. Appl. Cryst.*, 2009, **42**, 339.

8. G. M. Sheldrick, *Acta Cryst.*, 2015, **C71**, 3.

9. A. L. Spek, *Acta Cryst.*, 2015, **C71**, 9.

10. S. Parsons, H. D. Flack and T. Wagner, *Acta Cryst*., 2013, **B69**, 249.